Habitat highs and lows: Using terrestrial and UAV LiDAR for modelling avian species richness and abundance in a restored woodland

Shukhrat Shokirov, Tommaso Jucker, Shaun R Levick, Adrian D Manning, Timothee Bonnet, Marta Yebra, Kara N Youngentob

Habitat highs and lows: Using terrestrial and UAV LiDAR for modelling avian species richness and abundance in a restored woodland

Shukhrat Shokirov[1,2,3], Tommaso Jucker[4], Shaun R Levick[2], Adrian D. Manning[5], Timothee Bonnet[1], Marta Yebra[5,6], Kara N. Youngentob[1,5]

[1]Research School of Biology, Australian National University, Australia
[2]Commonwealth Scientific and Industrial Research Organization, Land and Water, Australia
[3]Department of Geodesy and Geoinformatics, Tashkent Institute of Irrigation and Agricultural Mechanization Engineers-National Research University, Uzbekistan
[4]School of Biological Sciences, University of Bristol, Bristol, UK
[5]Fenner School of Environment & Society, Australian National University, Australia
[6]School of Engineering, Australian National University, Australia

1. Abstract

Vegetation structure influences landscape use and habitat quality for many bird species. Owing to the difficulties associated with collecting structural data from traditional field measurements, numerous studies have investigated the utility of Light detection and ranging (LiDAR) for providing landscape-scale structural information that may be useful for exploring animal-habitat associations. Notably, almost all of these studies have involved the use of LiDAR from airborne rather than terrestrial platforms. However, vegetation metrics that might be important for explaining bird species occurrence and diversity, such as understory vegetation complexity and overall vegetation volume, may be partially obscured from airborne sensors by tree canopy cover. These challenges might be overcome by terrestrial and UAV LiDAR sensors that can provide detailed information of understory forest strata. For the first time, we collected terrestrial LiDAR (TLS) and unoccupied aerial vehicle LiDAR (ULS) data in a woodland landscape to compare the ability of both sensors to identify relationships among vegetation structural metrics and bird species richness and abundance. Overall, TLS and ULS models provided similar results based on the sampling methodology we used for LiDAR data collection in an open woodland landscape. Canopy roughness, ground vegetation vertical complexity, total vegetation volume and canopy height derived from these sensors were among the most common significant variables in explaining avian diversity and

individual species abundance. Individual species abundance models provided better prediction power (up to R^2 = 0.82 (TLS) and R^2 = 0.83 (ULS)) than bird community abundance by functional guilds (up to R^2 = 0.40 (TLS), R^2 = 0.41 (ULS)) and overall bird abundance (R^2 = 0.10 (TLS), R^2 = 0.16 (ULS)), species richness (R^2 = 0.14 (TLS), R^2 = 0.14 (ULS)) and diversity (R^2 = 0.17 (TLS), R^2 = 0.16 (ULS)). Additionally, we found that several vulnerable bird species are strongly associated with LiDAR structural variables, which may assist with habitat assessment and conservation management.

Keywords: TLS, laser scanning, birds, remote sensing, habitat modelling, Australia, vegetation structure

2. Introduction

Vegetation structure is the horizontal and vertical arrangement of plants across the landscape (Davies and Asner 2014; Verschuyl et al., 2008). Vegetation structural complexity and heterogeneity have been shown to have a positive relationship to biodiversity because they create a greater variety of microclimate and microhabitats that produce more food and cover for a range of species (Verschuyl et al., 2008). Previously, a number of studies have identified strong relationships between bird diversity and abundance and vegetation structure across different layers of vegetation (Kikkawa 1982; MacArthur 1961; Sekercioglu 2002; Stanley and Herman 1974). However, traditional methods to measure vegetation structure can be very time consuming and are often limited to point sampling a subset of the landscape (David et al., 2010; James and Shugart Jr 1970; Zehm et al., 2003).

Light Detection and Ranging (LiDAR) remote sensing technology can provide high-resolution topographic maps and information on vegetation height, cover, volume and complexity with a high level of detail and accuracy across landscapes (Bergen et al., 2009; Lefsky et al., 2002; Levick et al., 2019). Unlike passive sensors that depend on sun light reflected from objects, LiDAR uses a laser pulse emitted from the sensor. The reflected light is detected and digitized by the sensor creating a record of returns that are a function of the distance between the sensor and the reflected object (Anderson et al., 2016; Goetz et al., 2007; Lefsky et al., 2002). LiDAR sensor platforms can be terrestrial (Terrestrial Laser Scanner - TLS), mobile,

UAV (Unoccupied Aerial Vehicle) laser scanner (ULS), airborne (Airborne Laser Scanner - ALS) or satellite based (Sumnall et al., 2016; Vierling et al., 2008).

Vegetation structural metrics derived from LiDAR data have been widely used to investigate animal-habitat relationships, with a particular focus on birds (Bradbury et al., 2005; Eldegard et al., 2014; Goetz et al., 2007; Müller et al., 2010). Goetz et al. (2007) found that LiDAR derived canopy height distribution variables were a stronger predictor of bird species richness in temperate forest ecosystems than a commonly used vegetation index, Normalized Difference Vegetation Index (NDVI) derived from Landsat imagery. Various LiDAR-derived vegetation height, complexity and volume metrics are significantly correlated to bird species presence, diversity and abundance in many different forest environments (Clawges et al., 2008). Forest songbird species richness by different functional guilds also has been predicted from LiDAR-derived canopy and mid-story height and mid-story density in mixed hardwood forest (Clawges et al. 2011). A review by Davies and Asner (Davies and Asner 2014) revealed that 23 avian studies found a positive relationship between species richness and abundance and canopy structural diversity and vertical distribution of vegetation. In particular, vegetation structural heterogeneity appeared to have a stronger relationship to bird observations than canopy cover alone (Davies and Asner 2014).

Notably, most of the studies that used LiDAR to investigate relationships between vegetation structure and habitat quality for birds have used airborne LiDAR (Carrasco et al., 2019; Eldegard et al., 2014; Sasaki et al., 2016). While airborne LiDAR sensors provide accurate information on canopy structure, they have limited penetration to the ground and mid layer vegetation because of occlusion from the upper canopy (Bakx et al., 2019; Crespo-Peremarch et al., 2020; LaRue et al., 2020). A recent review analyzed 50 papers on bird species distributions and species richness in relation to LiDAR-based vegetation variables (Bakx et al., 2019). It was found that most of the studies used low density ALS data, usually 10 points/m^2, which have limited penetration below the canopy, especially to ground layer vegetation. The authors recommended that future studies should focus on higher density point clouds that can capture more details below the canopy, as the lower strata of vegetation is also important for many bird species (Bakx et al., 2019). They also suggested that, in addition to the widely used horizontal and height diversity

vegetation metrics, future research should also consider vegetation volume in different strata, which can be calculated from voxelized point cloud. Voxelized point cloud are three-dimensional grids or “voxels” that are created from one or more LiDAR points (Sasaki et al., 2016).

ULS may be able to overcome some of the limitations of airborne LiDAR sensors, since it can provide higher point density and still collects data relatively quickly. Fritz et al. (2018) demonstrated the potential of this technology for identifying important structural characteristics that help explain landscape use by an alpine bird community; however, the use of ULS for modelling bird-habitat associations has not been widely explored (Acebes et al. 2021). Ground-based TLS is an alternative platform that can provide more detailed information on vegetation below the canopy of forests because it measures the vegetation from the ground level and typically with higher resolution than airborne sensors (LaRue et al., 2020). Depending on the vegetation height and density, TLS can still be limited by occlusions though, where vegetation or other landscape structural features block the field of view (Crespo-Peremarch et al., 2020; LaRue et al., 2020). TLS data is typically only applied to smaller areas (< 1 ha) because collection time is slower than ULS and airborne LiDAR data (Liang et al., 2016). However, where logistically feasible, TLS may offer some advantages for measuring some understory vegetation structural metrics that are known to be important predictors of bird habitat quality and the occurrence and diversity of bird species (Michel et al., 2008).

For the first time, we utilized high-density TLS and ULS LiDAR derived vegetation structural variables for modelling vegetation structural classes and avian abundance and diversity in an Australian woodland. Incorporating the suggestions of earlier studies to investigate high-density point clouds and to incorporate vegetation volume metrics from voxilized point-clouds (Bakx et al., 2019; Sasaki et al., 2016), we used the data from both sensors to test the following hypotheses:

(1) the high-density TLS point clouds will perform better for modelling overall bird abundance, species richness and diversity than lower density ULS point clouds;

(2) the relationship between vegetation structural data and particular bird species and groups will be modelled more accurately from the TLS platform for bird species

and guilds that are most associated with ground and mid-story vegetation layers and ULS for those that primarily use the canopy strata.

We anticipate that the outcomes of this study will be useful for conservation and management projects focused on identifying animal-habitat associations and establishing appropriate habitat structure for wildlife management.

3. Methods

Study area

The study area is in Mulligan's Flat (683 ha) and Goorooyarroo (702 ha) nature reserves (MFGO) in the north-eastern corner of the Australian Capital Territory (ACT), Australia (35°09' S - 149°09' E; Fig. 1). These two adjacent reserves were established in 1994 and 2006 respectively to conserve and restore a critically endangered grassy woodland ecosystem (Manning et al., 2011). The dominant overstory tree species include Blakely's Red Gum (*Eucalyptus blakelyi*), Yellow Box (*E. melliodora*), Red Stringy Bark (*E. machrorhyncha*), and Scribbly gum (*E. rossii*) with a relatively open midstory of primarily *acacia spp*. The grassy ground-layer vegetation is dominated by *Joycea pallida*, *Austrodanthonia spp*., *Themeda australis* and *Aristida ramose* (McIntyre et al., 2014; McIntyre et al., 2010; Shorthouse et al., 2012). Prior to becoming reserves, MFGO was leasehold grazing land with some areas of past cropping and pasture improvement (Manning et al., 2011; Shorthouse et al., 2012). The topography is gently undulating with a few hills and the elevation ranges from 650 m to 700 m. Average daily temperature in 2018 ranged from a minimum of 6.9˚C to a maximum of 22.0 ˚C, and mean annual rainfall was 472.0 mm (Bureau of Meteorology 2019).

The reserves are the location of a long-term ecological experiment the "Mulligans Flat – Goorooyarroo Woodland Experiment" (Manning et al., 2011) As part of this experiment, restoration treatments have been undertaken in an attempt to restore the function and biodiversity of the area, and feral predators and grazers have been excluded with fencing around the reserves (Manning et al., 2013). To monitor ecosystem recovery over time, animal and vegetation surveys are periodically conducted across 96, 1 ha permanent sites (200 m x 50 m). These sites are stratified across the reserves in 24 clusters that each include one of the four different vegetation structural classes: 1) high tree cover, high shrub cover (HTHS), 2) high

tree cover, low shrub cover (HTLS), 3) low tree cover, low shrub cover (LTLS), and 4) low tree cover, high shrub cover (LTHS) (Fig 1). The clusters are the key stratifying unit of this experiment and are defined as homogenous areas of vegetation structure and type (Manning et al., 2011). Each site is marked in the field along the long axis by plastic pegs at the 0 m and 200 m points, and with star pickets (A and B) at the 50 m and 150 m points (Manning et al., 2011).

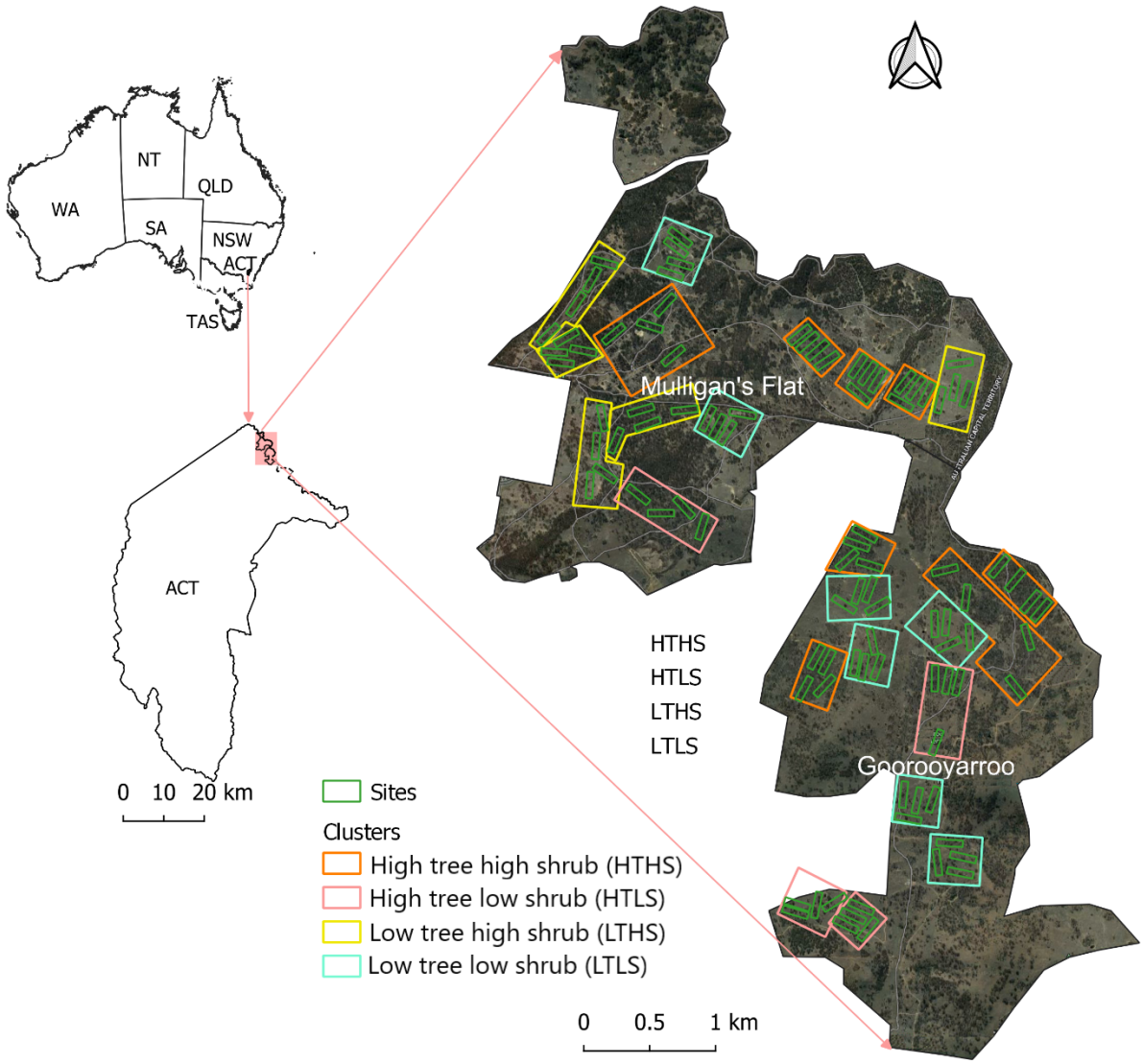

Figure 1. Map of study area in Mulligan's Flat-Goorooyarroo Woodland Sanctuaries (right panel), which is located in the north-east corner of the Australian Capital Territory (ACT), Australia. The green rectangles are 1 ha sites (n = 96) that are grouped by vegetation classes (clusters), which are outlined by the multi-color polygons. HTHS is high tree cover, high shrub cover, HTLS is high tree cover, low

shrub cover, LTHS is low tree cover, high shrub cover, and LTLS is low tree cover, low shrub cover.

3.1. Bird data collection

As part of long-term monitoring at MFGO, annual bird surveys have been conducted since 2005 at each site during two separate visits in October by different experienced bird observers using an acoustic and visual point count method (Manning et al., 2011). During the surveys, observers stand at the A and B star picket at the 50 m and 150 m position along the long axes of each site. The presence and abundance of birds in concentric bands (0 – 25 m, 25 – 50 m, 50 – 100 m and over 100 m and overhead) are recorded for ten minutes. Detailed information about bird survey methods are provided in (Manning et al., 2011). For this study, we used bird data collected from 2017, 2018, and 2019 because it is unlikely that the vegetation structure would have changed substantially in the period between LiDAR data acquisition in October-November 2018 and the bird counts from those adjacent years.

3.2. TLS data collection and post-processing

TLS data was collected in fine weather from 1 to 31 October 2018 with a Topcon GLS2000 (Topcon Corporation, Japan). The Topcon GLS2000 is a high-density laser scanner that emits near-infrared light (1064 nm) laser pulses at up to 120,000 laser pulses per second. The field-of-view of the scanner is 360° and 270° (horizontal and vertical direction, respectively). The beam diameter of the single pulse is 4 mm at 20 m. Information on a pilot study conducted to determine the number of TLS scans to be used for each site is provided in Appendix 1. We collected seven individual scans without co-registration in all 96, 1 ha sites for a total of 672 scans with 6 mm point spacing at 10 m from the scanner. The position of each scan was measured with a differential GPS (Trimble Geoexplorer 6000 series) and post-processing was performed using local base station data to improve the point location accuracy to approximately 50 cm (Shokirov 2021; Shokirov et al., 2020).

Point clouds from seven individual scan stations were then co-registered during post-processing using Multi-station Adjustment (MSA) plugin in RiScan Pro software (RIEGL Laser Measurement Systems GmbH). The MSA uses the iterative closest points (ICP) algorithm that minimizes the 3D distance between the identical points by translating and rotating the entire point cloud along X, Y, Z axes until the least minimum distance between the identical points from two datasets is achieved (Šašak et al., 2019). The exact procedure we followed is described in detail in Shokirov et al. (2021). Next, the point cloud from each site was georeferenced using DGPS locations of each scan position measured in the field and clipped to the spatial extent of each of the 96 sites. Point clouds were then subsampled into 1 cm spacing to homogenize the point distributions and duplicate points were removed using Cloud Compare (CloudCompare 2020).

3.3. ULS data collection and post-processing

We collected ULS LiDAR data across all of the 96, 1 ha sites in fine weather conditions from 7 to 14 November, 2018. The ULS LiDAR platform consisted of a quadcopter integrated with RIEGL miniVUX-1UAV LiDAR sensor (RIEGL Laser Measurement Systems GmbH, Austria) and APX INS/GNSS system (Trimble, USA). The flights were performed at approximately 80 m above the take off point with approximately 25.2 km/h speed, up to 5 returns per pulse, 100 kHz pulse repetition rate, and up to 100,000 measurements/second (Shokirov 2021; Shokirov et al., 2020). Maximum scan angle of the LiDAR sensor was approximately $\pm 60^0$ with swath width about 100 m. We used DJI ground station pro V2 to plan the flight missions (SZ DJI TECHNOLOGY CO. 2018). The ULS LiDAR sensor failed to collect data on two sites, which were excluded from further analysis of ULS and TLS data.

Data processing was done in RiPROCESS software suite by RIEGL which allowed us to bring in the trajectory data of the drone flight, align the flight paths, georeference the point cloud and then export it in LAS format. The trajectory data of the UAV LiDAR that was fed into RiPROCESS was generated using POSPAC UAV (Applanix) using the IMU/GNSS data from the drone and RINEX data from the base station which was obtained from the Gungahlin location of Smartnet global network. The ULS LiDAR data collected over the 94 sites were clipped by

corresponding polygons to create a separate point cloud for each site. Point spacing in ULS data across 94 sites ranged from 5 cm to 17 cm with an average of 10 cm. For this reason, we homogenized the point cloud with 10 cm spacing and removed duplicate points using Cloud Compare 2.10.2 (CloudCompare 2020).

3.4. Canopy height model

Point clouds were cleaned from noise points and classified into ground and non-ground points using *LAStools* (Isenburg 2012). We normalized point clouds by converting elevation values to height above ground values with *LAStools* (Isenburg 2012) (Fig. 2).

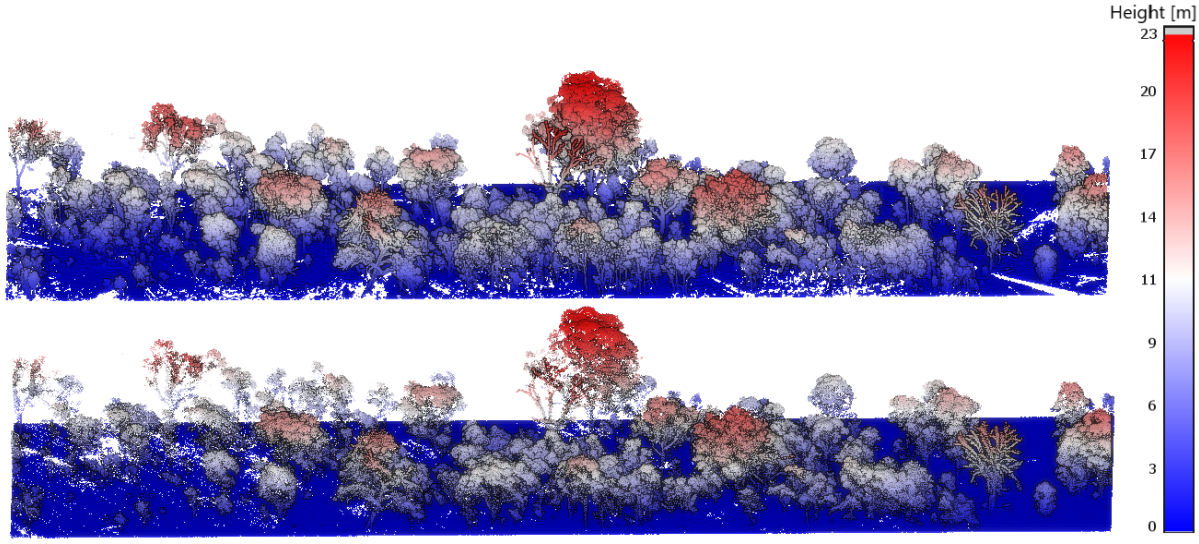

Figure 2. Normalized TLS (a) and ULS (b) point clouds of site GO72A-3 colored by height.

3.5. Calculating vegetation variables from the LiDAR datasets

Canopy metrics were calculated from points above 1.3 m (Table 1). Based on existing vegetation layer descriptions for eucalypt grassy woodlands (Department of Environment 2013), we divided the point cloud into three layers representing the ground layer (L1, points ≤ 1m), the mid-story (L2, 1m < points ≤ 10m) and the upper story (L3, points > 10m) (Fig. 3) and calculated additional vegetation metrics for each layer (Table 1). Vegetation volume was estimated by excluding ground points and

constructing 0.5 m voxels (volumetric pixels) from point clouds, with each voxel made of one or more points. A fraction of woody canopy cover for each site was calculated by creating 0.25 m grids from points above 1.3 m and dividing the sum of the areas of all pixels by the size of the total area of the site (200m×50m). A total of 37 metrics were computed with lidR package (Roussel, 2017). List of LiDAR–derived vegetation variables and descriptions are provided in Table 1.

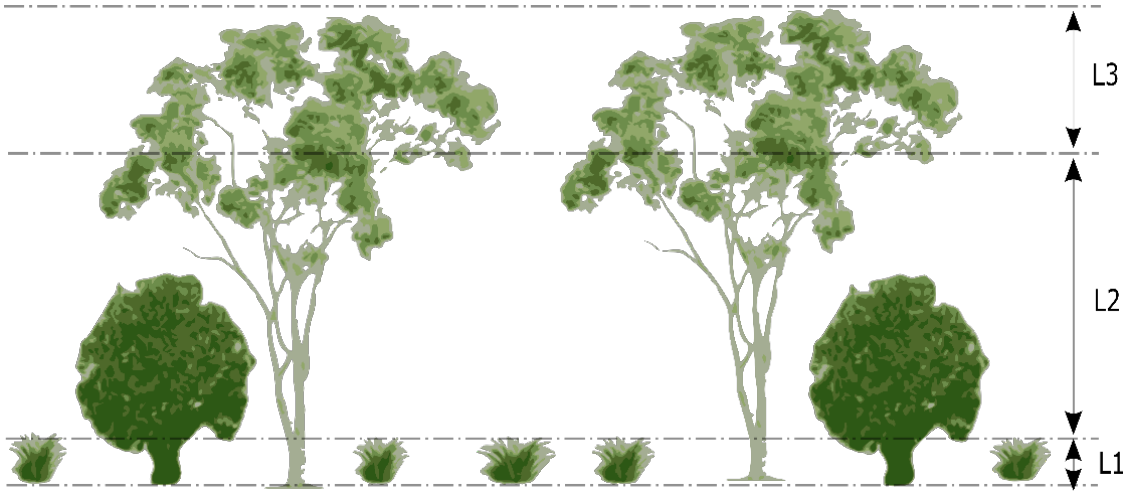

Figure 3. Vegetation layers: L1 - ground layer (points ≤ 1m), L2 - mid-story layer (1m <points ≤ 10m), L3 - upper story layer (points > 10m).

Table 1. Description of calculated vegetation structural variables from LiDAR dataset

Name of variable	Description
maxH	Maximum height of canopy (points > 1.3m).
meanH	Mean height of canopy (points > 1.3m).
stdH	Standard deviation of canopy height (points > 1.3m), which describes the variation in the canopy height.
skewH	Skewness of canopy height (points > 1.3m). Negative skewness means that the distribution is dominated by higher points (upper canopy is dominant) but a few extreme lower points. Positive skewness means that the distribution dominated by lower points (lower canopy is dominant) but a few extreme higher points.
kurH	Kurtosis of canopy height (points > 1.3m). Negative kurtosis means the distribution of points centered around the mean (mid-canopy is dominant). Positive kurtosis means the point

	distribution is heavy on tails and less around the mean (lower and upper canopy is dominant).
p_05, p_10, p_25, p_50, p_75, p_90, p_95, p_99	Canopy height percentiles (points > 1.3m). Canopy height percentiles are the height below which a specified percentage of total point clouds were located. For example, p_05 = 2 m means that 5% of vegetation points are found below 2 m.
vci_2m, vci_5m, vci_10m, vci_15m, vci_20m	Vertical complexity indexes (VCI) at 2m, 5m, 10m, 15m, 20m height bins, (points > 1.3m). Vertical complexity indexes (VCI) at 2m, 5m, 10m, 15m, 20m height bins, (points > 1.3m). $$VCI = (-\sum_{i=1}^{HB}[(p_i \ln(p_i)]))/\ln(HB)$$ Where *VCI* in a vertical complexity index, *HB* is the total number of height bins, and p_i is the proportional abundance of LiDAR returns in height bin *i*. A VCI value close to one indicates that most height bins have an equal amount of vegetation. VCI value decreases if the distribution of canopy in the height bin becomes more uneven (van Ewijk et al., 2011).
Cov	Fraction of canopy cover, (points > 1.3m).
height_cv	Coefficient of variation of height, (points > 1.3m). Indicates the canopy height variation.
canopy_roughness	Canopy roughness describes complexity/variability of canopy height (Herrero-Huerta et al., 2020) (points > 1.3 m). Higher variability in the canopy height provides higher roughness index and vice versa.
canopy_shannon	Normalized Shannon diversity index of canopy (Pretzsch 2009), (points > 1.3m). Indicates canopy height diversity.
Tvolume	Total vegetation volume (m^3) – number of 0.5 m^3 voxels divided by 8 (ground points excluded).
vlayer_L1	Vegetation volume (m^3) in 1st layer (points 0-1m¸ ground points excluded).

vlayer_L2	Vegetation volume (m^3) in 2st layer (points 1m-10m).
vlayer_L3	Vegetation volume (m^3) in 3st layer (points 10m and above).
meanH_L1, meanH_L2, meanH_L3	Mean height of 1st, 2nd, 3rd layer.
sdH_L1, sdH_L2, sdH_L3	Standard deviation of vegetation height in 1st, 2nd, 3rd layer.
roughness_L1, roughness_L2, roughness_L3	Roughness indexes of 1st, 2nd, 3rd layer (Jenness, 2004). Horizontal distribution of vegetation across different layers.
vci_L1, vci_L2, vci_L3	Vertical complexity indexes of 1st, 2nd, 3rd layer (van Ewijk et al., 2011). Vertical distribution of vegetation across different layers.

3.6. Statistical analysis

3.6.1. Bird data

We calculated bird abundance (maximum number of individual birds counted), species richness (cumulative total number of species), Shannon diversity index using "vegan" R package (Jari Oksanen 2019) and functional diversity indices including functional richness, functional evenness, functional divergence, functional dispersion and Rao's quadratic entropy for each site using "FD" package (Laliberté and Legendre 2010) in R language (R Core Team 2020). Shannon diversity index is used to characterize species diversity in a community (Morris et al., 2014). Functional richness is defined as the amount of niche space occupied by the species within a community. Functional evenness measures the regularity of the distribution of species abundances and dissimilarities in a functional space. Functional divergence is the degree to which abundance distribution in niche space maximizes divergence in functional characters within the community (Mason et al., 2005). Functional diversity indices quantify the trait diversity and act as a surrogate for the diverse ecological functions performed in the community. Rao's quadratic entropy measures the diversity of ecological communities and is based on the proportion of the abundance of species in a community and a measure of dissimilarity between the

species (Ricotta and Szeidl, 2009). The diversity of trait values within a community is therefore referred as either trait diversity or functional diversity (FD) (Karadimou et al., 2016). Bird guilds were assigned based on different functional traits (i.e., grassland specialist, water bird, woodland generalist, woodland specialist), nesting substrate (i.e., arboreal, ground, hollow, opportunistic, understory), foraging substrate (i.e., air, aquatic, arboreal, ground, opportunistic), and dispersion (low, partial, high) (Le Roux et al., 2018, Ikin et al., 2012).

3.6.2. Model selection process

A key stratifying unit of the sites established in our study area were the clusters, which were comprised of one of four vegetation types (HTHS, HTLS, LTLS, LTHS) (Manning et al., 2011). Although it was not the primary goal of the study, we first explored the ability of ULS and TLS data to correctly classify sites according to these vegetation categories. The outcomes from this classification exercise were used to select a modelling approach for relating the LiDAR structural data to the animal data. We used a multinomial regression model by means of “multinom” function in “nnet” R package (Venables and Ripley 2003) for this analysis. We tested two models, one based on the first four principle components from the PCA calculated from all TLS and ULS LiDAR variables (Appendix 2) and a model based on selected TLS and ULS LiDAR variables (3.6.3) to classify vegetation types. We also tested the performance of the four PCA components model and the selected variable model to predict overall bird abundance, species richness and diversity. However, we used the model type that most accurately classified the sites into their appropriate vegetation class for the full analysis of the bird data.

3.6.3. Variable selection process

For the selected variable model, we chose variables that were not highly correlated (0.7 maximum threshold), and this is in keeping with other studies (Dormann et al., 2013; Sasaki et al., 2016){Sasaki, 2016 #190}{Sasaki, 2016 #190}. Pearson correlation matrices of TLS and ULS variables are provided in Appendix 3 and Appendix 4, respectively. When selecting between two highly correlated variables, we attempted to select for the most ecologically meaningful variable (e.g. average height (*meanH*) and 75th percentile height (*p_75*) resulted in us selecting average

height). We also selected at least one variable from each strata of vegetation and several canopy metrics to cover all layers of vegetation in the landscape. The variable selection was conducted for each sensor, respectively. However, we gave preference to variables that were the same across sensors when the above criteria had been met. Although it was not our intention, our final variables consisted of the same 12 for each sensor. This was probably due to a combination of our selection method and the fact that the variables from the two sensors were highly correlated (Fig. 4), despite these sensors having different viewing geometry and point densities. All explanatory variables were standardized so that they have a mean of zero ("centering") and standard deviation of one ("scaling") (Becker et al., 1988). Additionally, a cross correlation matrix was calculated to examine the relationship between TLS and ULS variables.

3.6.4. Modelling bird diversity and abundance by guilds and individual species.

To evaluate which selected LiDAR based variables had the strongest relationship to bird abundance, species richness, species diversity, and functional diversity of birds across sites, we fitted linear mixed effects models. Correlations between individual bird abundance and bird abundance within functional guilds and vegetation structural metrics were evaluated using Poisson distribution generalized linear mixed effects models (GLMM) with glmer function in lme4 R package (Bates et al., 2015). Mixed models extend the basic linear model such that they recognize grouped or nested structures in data by random effects (Melin et al., 2018). In these models, predictor variables were the selected vegetation structural metrics (fixed effects) and twenty-four polygons (random effects), with each polygon containing four transects representing one of the four vegetation classes (see Fig. 1). Response variables were overall bird metrics, guilds and individual species abundance.

3.6.5. Examination of model fit

We used Residual Diagnostics for HierARchical Models (DHARMa) package (Hartig 2017) for examining the model fit, dispersion and zero-inflation. Marginal and

354 conditional R^2 were calculated to evaluate the proportion of variance explained by
355 fixed and mixed effects for models by species and guilds (Nakagawa et al., 2013).

356 To avoid model convergence issue, we retained the species or guilds that had at
357 least 10% count data across the sites. If the model convergence issue persisted, we
358 were able to resolve this by decreasing the number of fixed effects by removing
359 those with the lowest explanatory values. We considered a predictor to be significant
360 if the absolute value of its z-score was greater than 1.96, corresponding to a p-value
361 smaller than 0.05.

362 ## 4. Results

363 ### 4.1. Bird data

364 A total of 12117 bird observations (n = 5540 in Mulligan's Flat and n = 6577 in
365 Goorooyarroo) from 84 bird species were observed from the double surveys each
366 year across the three-year period from 2017 to 2019. A maximum of 238 birds and
367 36 species and a minimum of 42 birds and 10 species were counted in any one site
368 (Table 2). Most of the surveyed birds belong to the woodland specialist habitat class
369 (WS.HC, n = 8725), nested in hollows (Hol.Nest, n = 4668), foraged in the trees
370 (Arb.Forage, n = 6649) and displayed low dispersal (Low.Disp, n =8187) (Table 3).

371

372 Table 2. Basic statistics from bird data across sites. The table column headings are:
373 Abundance = bird abundance, SR = species richness, Bird_shannon = shannon
374 diversity, FRic = functional richness, FEve = functional evenness, FDiv = functional
375 diversity, FDis = functional dispersion, and RaoQ = Rao's quadratic entropy.

Statistics	Abundance	SR	Bird_shannon	FRic	FEve	FDiv	FDis	RaoQ
Maximum	238.00	36.00	3.22	0.09	0.82	0.96	0.29	0.09
Mean	126.22	21.97	2.63	0.01	0.67	0.87	0.24	0.07
Stdev	42.60	5.91	0.35	0.02	0.07	0.04	0.02	0.01
Median	121.50	22.00	2.69	0.01	0.67	0.87	0.24	0.07
Minimum	42.00	10.00	1.68	0.00	0.50	0.78	0.17	0.04

Table 3. Basic statistics about bird abundance within functional traits across sites. Habitat classes (GS.HC = grassland specialist habitat class, WB.HC = water bird habitat class, WG.HC = woodland generalist habitat class, WS.HC = woodland specialist habitat class), nesting substrate (Arb.Nest = arboreal nesting, Hol.Nest = hollow nesting, Usty.Nest = understory nesting, Opp.Nest = opportunistic nesting), foraging substrate (Air.Forage = airial foraging, Aqu.Forage = aquatic foraging, Arb.Forage = arboreal foraging, Grnd.Forage = ground foraging, Opp.Forage = opportunistic foraging), dispersion (Low.Disp – low dispersion, Partial.Disp – partial dispersion) groups.

Stats.	GS. HC	WB. HC	WG. HC	WS. HC	Arb. Nest	Grnd. Nest	Hol. Nest	Opp Nest	Usty. Nest	Air. Forage	Aqu. Forage	Arb. Forage	Grnd. Forage	Opp. Forage	Low. Disp	Partial. Disp
Sum	238	83	2868	8725	6174	44	4668	749	279	165	83	6649	2879	2138	8187	3722
Max	17	14	106	200	148	11	159	31	24	28	14	141	98	71	210	118
Mean	2.53	0.88	30.51	92.82	65.68	0.47	49.66	7.97	2.97	1.76	0.88	70.73	30.63	22.75	87.10	39.60
Stdev	3.14	2.35	20.33	34.72	28.19	1.59	32.00	7.93	4.81	4.08	2.35	27.53	18.98	13.64	34.44	23.14
Median	1.50	0.00	26.50	86.00	62.50	0.00	40.00	6.00	1.00	0.00	0.00	65.00	25.00	19.50	84.50	37.50
Min	0	0	2	28	11	0	5	0	0	0	0	19	5	1	29	3

4.2. Predicting vegetation classes from the LiDAR dataset

Multinomial regression models showed that selected LiDAR variables provided better accuracy in predicting vegetation classes than the first four PCA variables for both TLS and ULS data (Appendix 5. Table A5.1 and Table A5.2). Therefore, we decided to use selected variables over PCA variables as predictors in our models. For both TLS and ULS datasets, models were better at classifying HTHS and LTLS vegetation classes than HTLS and LTHS vegetation classes.

4.3. Selected variables

Our variable selection method resulted in 12 out of 37 LiDAR metrics being selected for the models. The Pearson correlation matrix showed that most of the TLS and ULS variables are strongly correlated to each other (r > 0.7) (Fig. 4). Only the L1 metrics and lower strata canopy metrics showed a weak correlation (r < 0.3) to each other. Basic statistics for these TLS and ULS variables are provided in Figure 5.

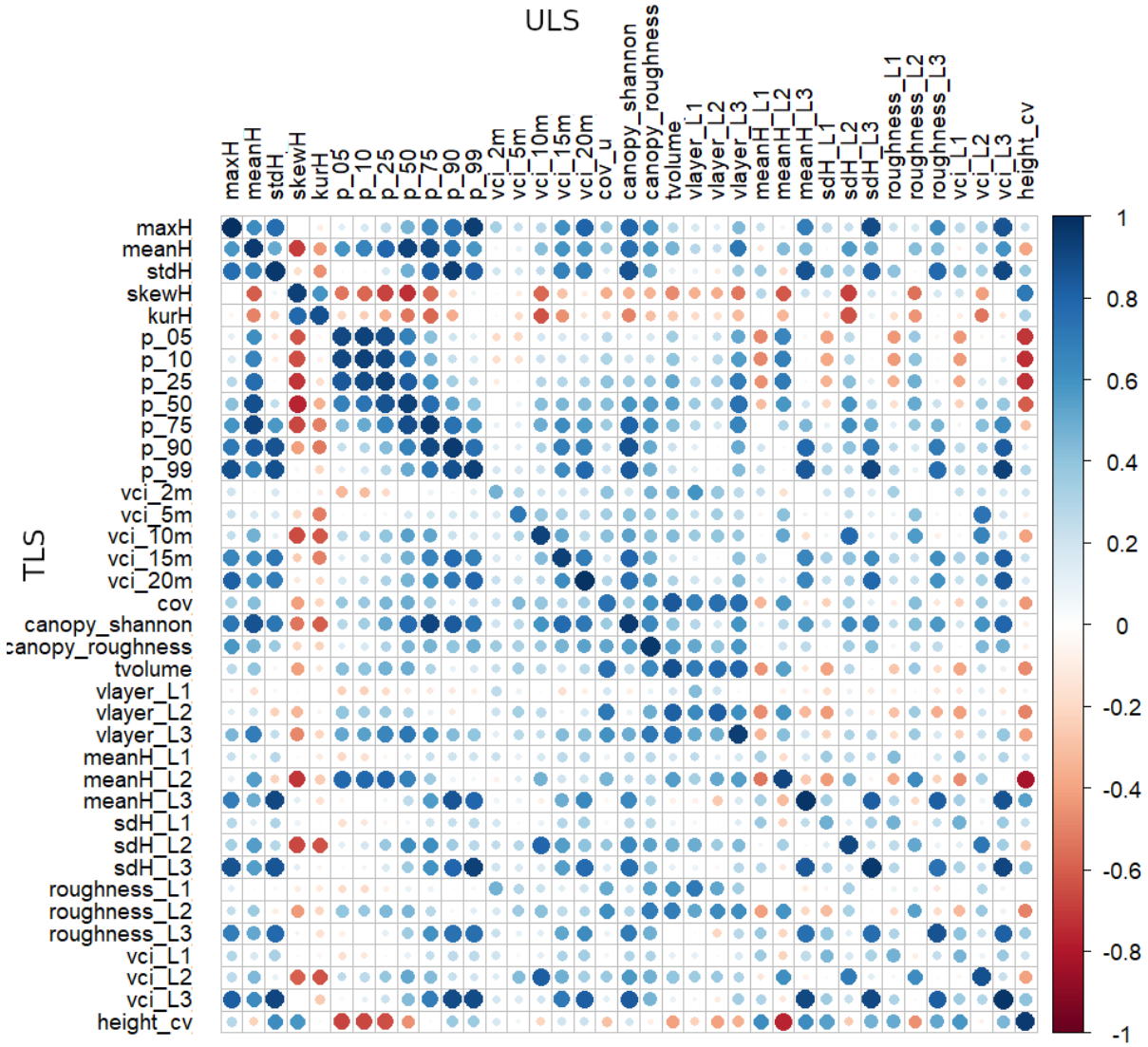

Figure 4. Correlation matrix of Terrestrial Laser Scanner (TLS) and Unoccupied Aerial Vehicle Laser Scanner (ULS) variables

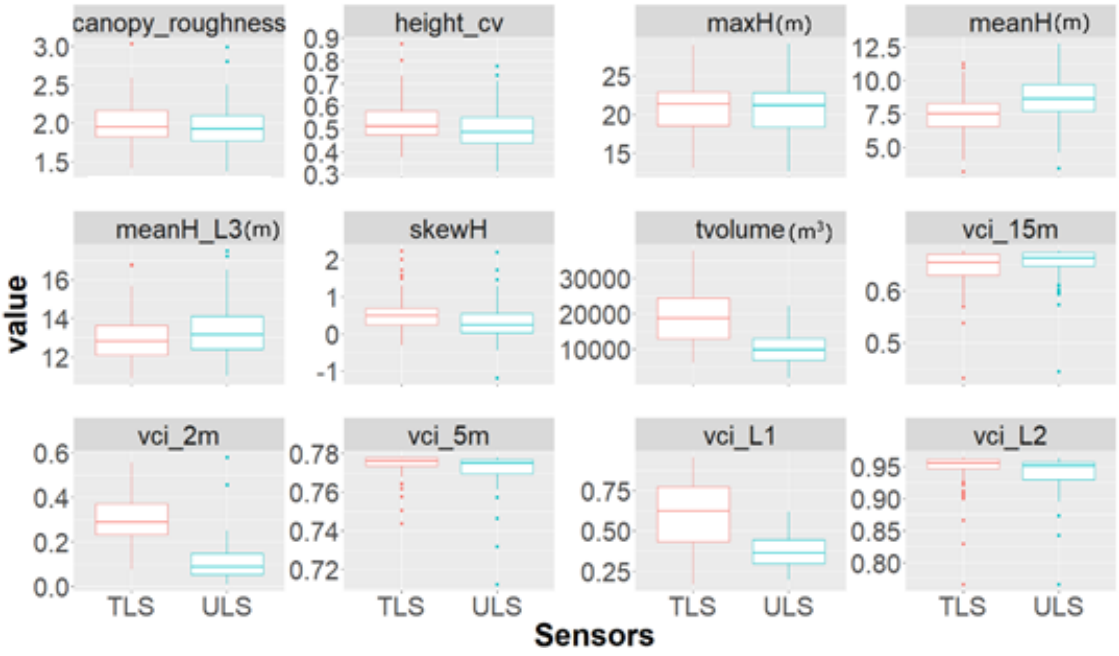

405

406 Figure 5. Boxplots represent the distribution of selected terrestrial laser scanner
407 (TLS) and unoccupied aerial vehicle laser scanner (ULS) variables. Upper, mid, and
408 lower horizontal lines of the box indicate 1th, median, and 3rd quartiles. Whiskers
409 extend to the highest and lowest extreme of observations, and the dots on the
410 whiskers are outliers

4.4. Overall bird abundance, species richness and diversity

The GLMM for the overall bird abundance did not show a significant relationship with any of the 12 selected variables from the ULS or TLS data (Appendix 6, "Abundance", Fig. 6). Bird species richness (*SR*) was positively related to several TLS-derived variables including *meanH*, and *skewH* and *height_cv* and negatively correlated to *meanH_L3*. However, *tvolume* was the only significant predictor among the ULS selected variables for predicting bird species richness (*SR*). Bird diversity (*Bird_shannon*) was positively influenced by TLS and ULS *meanH* and *tvolume*, and negatively influenced by *meanH_L3* (Appendix 6, "Bird_shannon, Fig. 6). Among the functional diversity indexes, functional evenness (*FEve*) was negatively correlated to only TLS-based *vci_15m*. However, *vci_15m* derived from TLS and ULS data was negatively related to functional divergence. Functional dispersion (*FDis*) and Rao's quadratic entropy (*RaoQ*) were negatively influenced by TLS and UAV – derived *vci_2m* and *vci_15m*, and positively related to ULS – based *vci_L1* (Appendix 6, Fig. 6). However, all these models showed relatively poor performance with explained variance between 10.0% and 20.0% (Appendix 6).

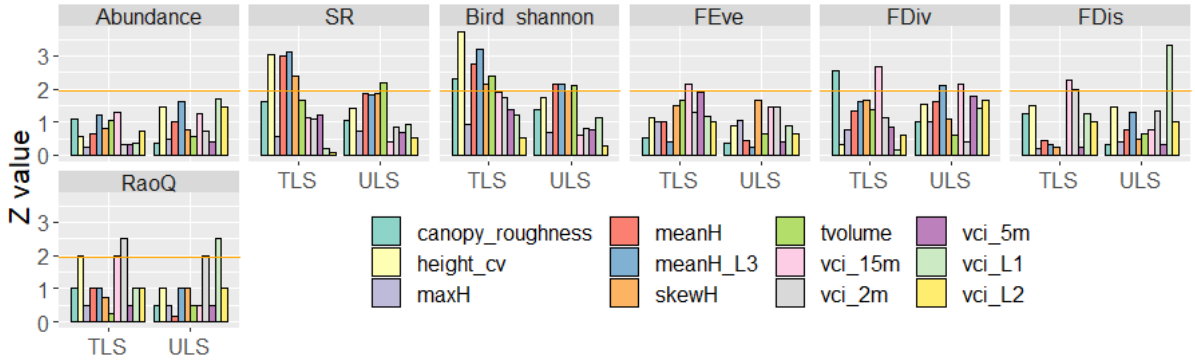

Figure 6. Plots illustrate the significance of predictor variables (by z value) for predicting overall bird abundance, species richness and diversity. Bars represent predictor variables. The horizontal orange line shows the significance threshold (z = 1.96, or $p < 0.05$) of predictors. The abbreviations are: FDis = Functional dispersion, FDiv = functional divergence, FEve = functional evenness, RaoQ = Rao's quadratic entropy, SR = species richness, TLS = terrestrial laser scanner, and ULS is unoccupied aerial vehicle laser scanner.

436

437 ### 4.5. Bird abundance within functional guilds

438 All of the 16 functional guilds (Table 3) were significantly correlated to one or more
439 LiDAR variables, and some guilds showed a stronger response to vegetation
440 structure than others (Appendix 7, Fig. 7). Models from TLS data explained between
441 8.5% and 39.9% (average of 22.6%) variability, and ULS models explained between
442 6.8% and 40.8% (average of 23.5%) variability in abundance of birds across
443 functional guilds.

444 The most robust TLS-based explanatory models were the water bird habitat class
445 (R^2=0.40) and aquatic foragers abundance (R^2=0.40), which were positively
446 correlated to *meanH*, *skewH* and *vci_5m*, and negatively correlated to *maxH and*
447 *meanH_L3*. The ground nesting guild model from TLS data explained substantial
448 variance (R^2 = 0.34), and was negatively influenced by *maxH* and positively
449 influenced by *skewH*, *tvolume* and *vci_L2*. The TLS-based opportunistic foraging
450 model was the third best at explaining variance in the data (R^2 = 0.31). That model
451 was negatively correlated to *maxH*, *meanH*, *skewH* and *height_cv* and strongly
452 positively correlated to *canopy_roughness* and *meanH_L3* (Appendix 7, Fig. 7).

453 The ULS-based models also performed best for aquatic foraging and water bird
454 habitat guilds (R^2 = 0.41), which were positively related to *vci_5m*, *vci_15m* and
455 *vci_L1*. The next best performing ULS guild model was for woodland generalist
456 abundance (R^2 = 0.37) and was positively associated with *maxH* and *vci_L1*. The
457 ULS model also explained substantial variance in abundance of ground nesting birds
458 (R^2=0.35), which were positively influenced by *meanH* and *skewH*, but negatively
459 related to *maxH* (Appendix 7, Fig. 7).

460 Canopy roughness (*canopy_roughness*) was the best predictor variable for the TLS-
461 based models with a significant correlation to 10 functional guilds followed by *skewH*,
462 *maxH* and *meanH* height of canopy and *meanH_L3* (Fig. 7). The best predictor
463 variables for ULS-based models were *vci_5m*, which was significantly correlated to 9
464 guilds, *maxH, canopy_roughness* and *vci_L1* (Fig. 7).

465

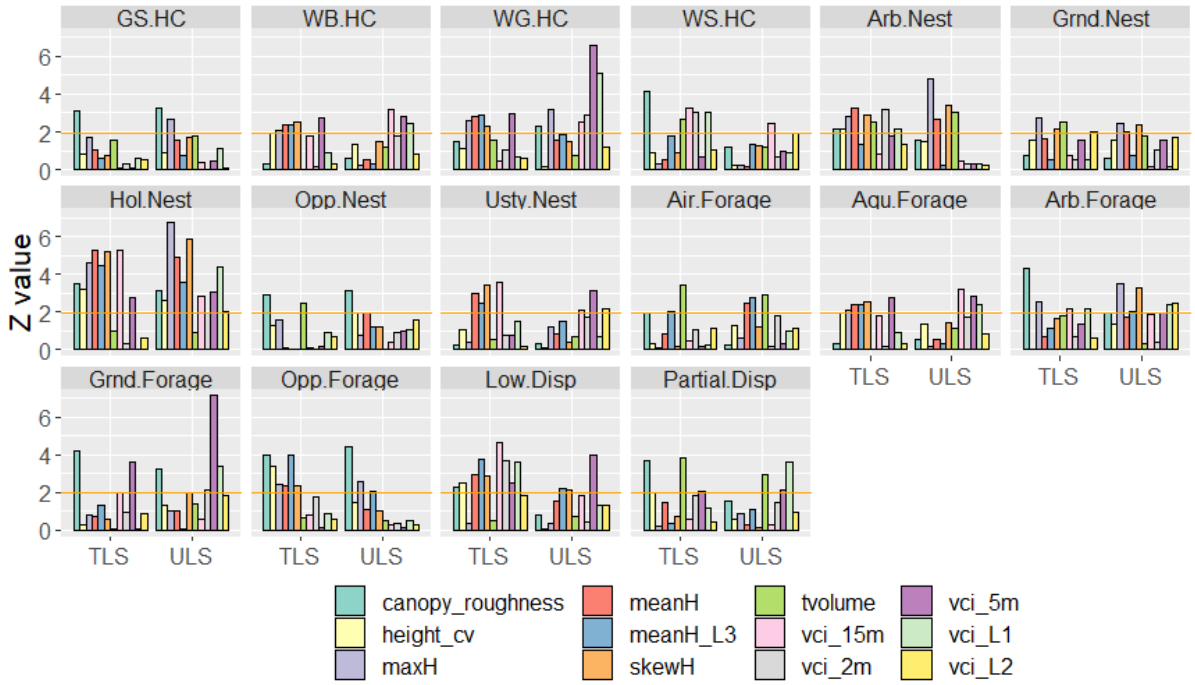

Figure 7. Plots illustrate the significance of predictor variables (by z value) from terrestrial laser scanner (TLS) and unoccupied aerial vehicle laser scanner (ULS) for predicting bird abundance by functional guilds. Bars represent predictor variables. Horizontal orange line shows the significance threshold ($z = 1.96$, or $p < 0.05$) of predictors. The abbreviations are: habitat classes (GS.HC = grassland specialist, WB.HC = water bird, WG.HC = woodland generalist, and WS.HC = woodland specialist), dispersal (Low.Disp = low, and Partial.Disp = partial), nesting substrate (Arb.Nest = arboreal, Hol.Nest = hollow, Usty.Nest = understory, and Opp.Nest = opportunistic), foraging substrate (Air.Forage = air, Aqu.Forage = aquatic, Arb.Forage = arboreal, Grnd.Forage = ground, and Opp.Forage = opportunistic).

4.5.1. Individual bird species abundance

Abundance of forty-nine out of fifty-one bird species responded to TLS and ULS – derived vegetation structural variables (Appendix 8). Only Grey Shrike Thrush and Pallid Cuckoo abundance showed no relationship to any TLS or ULS LiDAR structural variables. For the TLS-based models, *canopy_roughness* was significantly related to the abundance of 16 bird species, followed by *tvolume*, which was related to the abundance of 15 bird species (Fig. 8). In the ULS models, *vci_L1* related to bird species abundance more than any other variable (22 bird species), followed by

canopy_roughness (17 bird species) (Fig. 8). Explained variance of TLS models ranged from 4.2% to 81.7% (average of 31.1%). Similarly, ULS-models explained 4.9% to 83.4% (average of 30.5%) of variation in bird species abundance.

Figure 8. Plot illustrates the significance of predictor variables (by z value) from terrestrial laser scanner (TLS) and unoccupied aerial vehicle laser scanner (ULS) for predicting individual bird species abundance. Bars represent predictor variables. Horizontal orange line shows the significance threshold ($z = 1.96$, or $p < 0.05$) of predictors.

The model for Nankeen Kestrel abundance was the best performing TLS model ($R^2 = 0.82$), and was strongly correlated to *vci_15m*, *canopy_roughness*, *meanH_L3* and *vci_L2* and negatively related to *meanH* and *tvolume* (Appendix 8, Fig 8). The second best TLS model was Spotted Pardalote abundance ($R^2 = 0.77$), which was correlated to *maxH*, *meanH*, *skewH* and *tvolume*. White Throated Treecreeper abundance was also strongly related to TLS LiDAR-derived vegetation structure ($R^2 = 0.74$) and had a positive relationship to *skewH*, *vci_15m*, *tvolume* and *vci_L2*, and a negative relationship with *maxH* and *vci_5m* (Appendix 8, Fig 8).

The best performing ULS model was for Varied Sittela abundance ($R^2 = 0.83$), which was explained by *maxH*, *meanH*, *skewH* and *meanH_L3*. The White Throated Treecreeper abundance model ($R^2 = 0.78$) showed significant correlation with *meanH*, *skewH*, *canopy_roughness*, *meanH_L3* and *vci_L1*. Likewise, the Sacred Kingfisher abundance model explained 76.2% variance and was related to *maxH*, *meanH*, *skewH*, *meanH_L3*, *vci_L1* and *height_cv* (Appendix 8, Fig. 8).

Overall, TLS and ULS data produced very similar results in predicting individual bird species abundance, and this was demonstrated by the linear relationship between the explained variances of TLS and ULS models (Fig. 9).

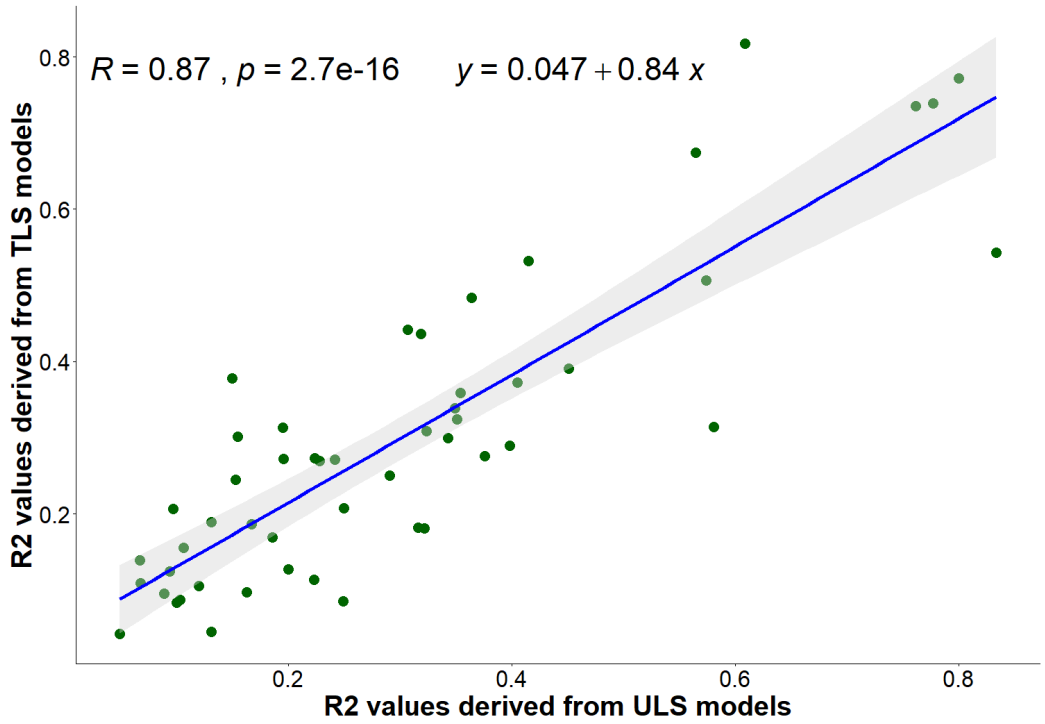

Figure 9. The relationship between explained variance (R2) calculated from TLS and ULS based Poisson distribution mixed model for predicting individual bird species abundance.

5. Discussion

This is the first study that uses both ULS and TLS data for investigating relationships between a wide range of bird population data and vegetation structure in a woodland landscape. It is also the first study in Australia to model avian abundance and species richness using LiDAR data. Overall (combined species) bird abundance was not significantly related to any TLS or ULS LiDAR-derived variables, and this may be due to the number of different bird species that occupied a wide variety of structural niches in the landscape (Lesak et al., 2011). Models for predicting bird species richness, diversity and abundance within functional guilds performed better than overall bird abundance.

Some individual bird species abundance models were able to explain a very large amount of variability in abundance of particular species, which is promising for using this data for habitat assessments and improving our understanding of habitat requirements for threatened species in particular. Canopy roughness, vertical complexity of the first layer, total vegetation volume and canopy height were the

variables that were most strongly associated with bird community and individual species abundance. Our assumption that higher density LiDAR point clouds from the TLS platform would create better models than the lower density, airborne ULS data was not supported by our data. This was likely influenced by low-lying occlusions in the data that were more substantial for the TLS than the ULS owing to the positioning of the sensors and the characteristics of the woodland landscape (Olschofsky et al., 2016). As a result, the ULS generally provided better results for predicting the abundance of individual bird species and guilds that forage on the ground than the TLS based on our methodology. We discuss the overall finding in more detail below and provide recommendations for future research.

5.1. Overall bird abundance, species richness and diversity

The lack of significant relationships between TLS and ULS structural metrics and overall bird abundance may be due to contrasting habitat requirement across the large suite of different species included in the total abundance tally (Wiens and Rotenberry, 1981). Models for predicting overall bird species richness did find significant relationships to some variables but these were dependent on the data source (TLS or ULS). Species richness was positively related to TLS canopy height diversity and upper canopy height. The only ULS predictor that was significantly related to bird species richness was the total volume of vegetation. The TLS sensor may be able to capture more meaningful structural variation below the canopy for birds than the ULS data owing to the positioning of the sensor under the canopy. Overall species diversity models from TLS and ULS data provided similar results with canopy height and total volume being strongly related to the bird diversity indices, but *height_cv* was only significant in TLS-based metrics (Appendix 6). This further supports the idea that the TLS sensor was able to capture canopy height variation in a more meaningful way for bird habitat quality, probably owing to the positioning of the sensor (Ashcroft et al., 2014; Blakey et al., 2017). Nonetheless, the higher density TLS data did not perform better than the ULS data in terms of overall ability to explain variance in this data. Therefore, our first hypothesis that high density TLS LiDAR point clouds will perform better for modelling overall bird abundance, species richness and diversity than lower density ULS point clouds was not supported with the number of TLS scans per site that we collected.

Generally, our results from species richness and diversity models agree with relationships identified in previous studies (Clawges et al., 2008; Lesak et al., 2011; Sasaki et al., 2016). Clawges et al. (2008) found a significant correlation between ALS LiDAR-derived canopy height diversity and bird species diversity. Similarly, ALS LiDAR – derived canopy height and mid-story density and height has been associated with song bird species richness (Lesak et al., 2011). Notably, these studies reported relatively low overall explained variance (R^2 <= 0.2), which is also in keeping with our findings. The typically low explained variance for community level data (e.g., bird species richness and diversity) in these models may be due to a mismatch in scale, since some of the bird species frequently use landscape areas beyond the site level that have different overall structural characteristics. Bird occurrence and habitat relationships can be scale-dependent (Seavy et al., 2009; Weisberg et al., 2014). Weisberg et al. (2014) investigated multiscale habitat heterogeneity and bird occurrence using LiDAR data, and they found the strongest associations at a 200 m (4 ha) scale and the weakest associations at a 50 m (0.25 ha) scale. A similar study on multiscale analysis using LiDAR derived canopy height measurements (Seavy et al., 2009) found that specific bird species responded differently to vegetation structure at different spatial scales. Future studies should revisit this dataset at a variety of scales.

5.2. Modelling bird abundance within functional guilds

All of the functional guilds that we analyzed were significantly related to LiDAR derived vegetation structural metrics. Generally, TLS and ULS data achieved similar results in predicting functional guild abundance (average R^2 = 0.23). A few earlier studies have also used remote sensing to investigate relationships between bird functional guilds and vegetation structure, but they used species richness within guilds, rather than species abundance within guilds (Lee et al., 2017; Lesak et al., 2011). For example, ALS-derived vegetation measures have been used for estimating songbird species richness by nesting, foraging and edge preferring guilds (Lesak et al., 2011). In that study, models using structural metrics from ALS data explained between 7.0% and 16.1% of the variance in species richness in nesting guilds, whereas our study explained between 8.5% and 33.7% (TLS) and 6.8% and 35.5% (ULS) variance in the abundance of birds from various nesting guilds. Another study also found significant relationships between canopy height and density

variables and foraging guilds (Lesak et al., 2011). Our models showed that bird abundance by functional guilds is often influenced by canopy height variables, canopy roughness and vertical complexity of vegetation in the ground layer. Notably, the ULS models found strong correlations between ground foraging guilds and ground-layer vegetation structure, but the TLS models did not show this relationship. This indicates that the ULS may capture more structural heterogeneity due to less occlusion in the ground-layer in an open woodland than the TLS. As a result, a portion of our second hypothesis that overall, TLS data from the seven scan stations per site will perform better than ULS data in predicting avian functional guild abundance for ground foraging or low nesting species is rejected.

5.3. Modelling individual bird species abundance

The relationship between specific vegetation structural metrics and the abundance of certain bird species may be useful for future management and conservation efforts, particularly for vulnerable species. In many cases, the link between the structural metrics and specific bird species can be easily explained by their habitat preference, lending more weight to this relationship. For example, we found that the abundance of the vulnerable Superb Parrot (*Polytelis swainsonii*, Nature Conservation Act 2014) is positively influenced by TLS-derived maximum height of trees and ULS-derived maximum height of trees and the complexity of the first layer vegetation and negatively influenced by horizontal distribution of canopy (*canopy roughness*). Separate studies have found that Superb Parrots use large trees for nesting and breeding and ground vegetation for foraging (Manning et al., 2004a). In addition to the Superb Parrot, our LiDAR-derived structural models also performed very well in predicting the abundance of two other threatened species, the White-winged Triller (*Lalage tricolor*, Nature Conservation Act 2014), and the Varied Sittella (*Daphoenositta chrysoptera*, Nature Conservation Act 2014).

Some woodland sensitive birds also responded to the LiDAR derived vegetation structural metrics. For example, the Brown Thornbill (*Acanthiza pusilla*) is a species found in sparse eucalypt woodlands (Stagoll et al., 2010) and its abundance was negatively correlated to canopy roughness and mean height of canopy (Appendix 8, Fig 8). Prior studies found that Noisy Miners (*Manorina melanocephala*) are less likely to occur in areas with high shrub cover (Crates et al., 2018; Montague-Drake et al., 2011; Val et al., 2018), and our noisy miner model also found a significant

negative relationship to shrub layer vegetation (Appendix 8). This finding suggests that managing landscapes to increase shrub cover should reduce the negative impact of this aggressive species, which is native, but often overabundant in human modified landscapes (Debus 2008).

On the other end of the extreme, we found no relationship between our site-level structural variables and the abundance of the Grey Shrike-thrush (*Colluricincla harmonica*) or Pallid Cuckoo (*Cacomantis pallidus*). These common species are widely distributed across Australia and use habitat at large spatial scales and across a wide range of landscape types (BirdLife 2020). If relationships between these species and specific structural variables are to be found, then it is more likely to be at larger spatial scales than our 1 ha site-level metrics. Overall though, the individual bird species models from both TLS and ULS performed better than the community-based models, and that's notable because habitat is a species specific concept (Betts et al., 2014; Manning et al., 2004b). In trying to understand the structural requirements of wildlife using LiDAR data, it may be best to focus on individual species rather than overall abundance or diversity (Manning et al., 2004b). Contrasting requirements from multiple species may frustrate attempts to model relationships to structural vegetation data (Halstead et al., 2019).

Out of 51 bird species, ULS ground-layer vegetation structure was important for 22 species, compared to 13 species for the TLS models (Appendix 8, Fig. 8). The abundance of ground foraging birds such as Yellow-rumped Thornbill (*Acanthiza chrysorrhoa*), Yellow-faced Honeyeater (*Lichenostomus chrysops*), Sulphur-crested Cockatoo (*Cacatua galerita*), Superb Parrot (*Polytelis swainsonii*), Red-rumped Parrot (*Psephotus haematonotus*), Little Corella (*Cacatua sanguinea*) were significantly influenced by ground layer vegetation complexity for ULS but not TLS data (Appendix 8, Fig 8). This might be related to the occlusion of TLS laser pulses by ground vegetation (LaRue et al., 2020) and the ability of ULS to capture ground vegetation structure in an open woodland due to the open canopy architecture of this landscape (Yebra et al., 2015). As expected though, we did find that some species that depend on canopy strata such as Buff-rumped Thornbill (*Acanthiza reguloides*), Eastern Rosella (*Platycercus eximius*), Red-rumped Parrot (*Psephotus haematonotus*) and Red Wattlebird (*Anthochaera carunculata*) were significantly associated with more ULS canopy variables than TLS. For these reasons, our

second hypothesis is partially supported because the relationship between vegetation structural data and particular bird species was modelled more accurately from the ULS data for species that primarily use the canopy strata.

5.4. TLS and ULS datasets

Although we compared the performance of TLS and ULS data in modelling bird-habitat associations, it is important to recognize that we collected 7 scans of TLS data in each 1 ha site, and this is a relatively low number of scans compared to recent studies that acquired more than 16 scans in 1 ha sites (Levick et al., 2021; Wilkes et al., 2017). However, most of those studies collected data over only a few hectares in total, which makes more scans per ha and associated post-processing feasible. Increasing the number of TLS scans across our 96, 1 ha sites would increase the time required for data collection, making it less comparable in effort to the ULS data. However, more TLS scans would decrease incident angle (i.e., the angle between the incoming laser pulse and surface), which would capture dense vegetation and ground more completely, substantially reducing occlusions (Soudarissanane et al., 2009).

Topcon GLS2000 is a single return LiDAR sensor, and a multiple return TLS sensor would have been able to penetrated farther into vegetation (Wilkes et al., 2017). The ability of the ULS sensor to record multiple returns, as well as its smaller incident angle, provided advantages over the TLS. Higher point density TLS LiDAR data in itself does not offer an advantage over lower point density ULS data if the coverage is less complete and the landscape type allows a ULS sensor to view lower strata vegetation to successfully model structural associations between plants and animals.

5.5. Conclusions

Mixed models showed strong relationships between vegetation structural metrics derived from TLS and ULS sensors and the abundance of many individual bird species and their functional guilds. This type of data can be useful for identifying habitat requirements for a variety of bird species (Graf et al., 2009). The performance of ULS models and the speed at which ULS data can be collected relative to TLS sensors is particularly promising for this application. Understanding the landscape-scale that species use and matching this to the scale of LiDAR

structural metrics may improve our ability to identify relationships between remotely sensed vegetation structure and wildlife (Seavy et al., 2009).

Acknowledgements

We thank all of our volunteers; L. McGibbon, E. Wu, R. Stainer, P. Hopkins, K. Spooner, Jackie, K. Subasinghe, M. Folkard, Z. Xie, Karen, Prasanna, W. Wang, D. Muthiah, B. Candice, M. Jenkins, N. Butcher, and S. Zong for their hard work during data collection. We express our gratitude for Paul B. Yeoh from CSIRO who helped to collect UAV LiDAR dataset. Thank you to J. Newport for supplying data sets and coordinating bird surveys and Canberra Ornithologists Group and many volunteers who have undertaken bird surveys. Thanks to R. Clark and M. Welvaert for additional statistical support and consultation, K. Schiphof for editorial assistance, and two anonymous reviewers whose helpful comments greatly improved our research presentation. We are grateful for advice and assistance provided by ACT Government staff, especially M. Snape, and Woodlands and Wetlands Trust staff. Avian data were collected with the support of the Mulligans Flat – Goorooyarroo Woodland Experiment, and an Australian Research Council Linkage grant (LP140100209). This study was also supported by a grant from the Australian Research Council (DE150101870) and a Centre for Biodiversity Analysis Ignition Grant (ANU). Bird surveys were covered by ANU ethics Protocols C.RE.44.05, C.RE.59.09, F.ES.10.10, A2011/017, A2014/35, A2017/33 and A2020/40; and ACT project licenses LT2005201, LT2007279, LT2009347, LT2010417, LT2014769, LT2015834, LT2016905 and LT2017959.

References

Anderson, K., Hancock, S., Disney, M., Gaston, K.J., Rocchini, D., & Boyd, D. (2016). Is waveform worth it? A comparison of LiDAR approaches for vegetation and landscape characterization. *Remote Sensing in Ecology and Conservation, 2*, 5-15

Acebes, P. Lillo, P. Jaime-González, C. Disentangling LiDAR Contribution in Modelling Species–Habitat Structure Relationships in Terrestrial Ecosystems Worldwide. A Systematic Review and Future Directions. *Remote Sensing,* 2021, 13, 3447

Ashcroft, M.B., Gollan, J.R., Ramp, D., & Kriticos, D. (2014). Creating vegetation density profiles for a diverse range of ecological habitats using terrestrial laser scanning. *Methods in Ecology and Evolution, 5*, 263-272

Bakx, T.R.M., Koma, Z., Seijmonsbergen, A.C., Kissling, W.D., & Zurell, D. (2019). Use and categorization of Light Detection and Ranging vegetation metrics in avian diversity and species distribution research. *Diversity and Distributions, 25*, 1045-1059

Bates, D., Mächler, M., Bolker, B., & Walker, S. (2015). Fitting Linear Mixed-Effects Models Using lme4. *Journal of Statistical Software, 67*, 48

Becker, R., Chambers, M., & Wilks, A.R. (1988). *The New S Language: A Programming Environment for Data Analysis and Graphics*. Wadsworth & Brooks/Cole Advanced Books & Software

Bergen, K.M., Goetz, S.J., Dubayah, R.O., Henebry, G.M., Hunsaker, C.T., Imhoff, M.L., Nelson, R.F., Parker, G.G., & Radeloff, V.C. (2009). Remote sensing of vegetation 3-D structure for biodiversity and habitat: Review and implications for lidar and radar spaceborne missions. *Journal of Geophysical Research: Biogeosciences, 114*

Betts, M.G., Fahrig, L., Hadley, A.S., Halstead, K.E., Bowman, J., Robinson, W.D., Wiens, J.A., & Lindenmayer, D.B. (2014). A species-centered approach for uncovering generalities in organism responses to habitat loss and fragmentation. *ECOGRAPHY, 37*, 517-527

BirdLife, A. (2020). BirdLife Australia

Blakey, R.V., Law, B.S., Kingsford, R.T., & Stoklosa, J. (2017). Terrestrial laser scanning reveals below-canopy bat trait relationships with forest structure. *Remote Sensing of Environment, 198*, 40-51

Bradbury, R.B., Hill, R.A., Mason, D.C., Hinsley, S.A., Wilson, J.D., Balzter, H., Anderson, G.Q.A., MARK J. Whittingham, M.J., Davenport, I.J., & Bellamy, P.E. (2005). Modelling relationships between birds and vegetation structure using airborne LiDAR data a review with case studies from agricultural and woodland environments. *British Ornithologists' Union, IBIS, 147*, 443–452

Bureau of Meteorology, A. (2019). Climate summaries archive.

Carrasco, L., Giam, X., Papeş, M., & Sheldon, K. (2019). Metrics of Lidar-Derived 3D Vegetation Structure Reveal Contrasting Effects of Horizontal and Vertical Forest Heterogeneity on Bird Species Richness. *Remote Sensing, 11*, 743-762

762 Clawges, R., Vierling, K., Vierling, L., & Rowell, E. (2008). The use of airborne lidar
763 to assess avian species diversity, density, and occurrence in a pine/aspen forest.
764 *Remote Sensing of Environment, 112*, 2064-2073

765 CloudCompare (2020).

766 Crates, R., Terauds, A., Rayner, L., Stojanovic, D., Heinsohn, R., Wilkie, C., &
767 Webb, M. (2018). Spatially and temporally targeted suppression of despotic noisy
768 miners has conservation benefits for highly mobile and threatened woodland birds.
769 *Biological Conservation, 227*, 343-351

770 Crespo-Peremarch, P., Fournier, R.A., Nguyen, V.-T., van Lier, O.R., & Ruiz, L.Á.
771 (2020). A comparative assessment of the vertical distribution of forest components
772 using full-waveform airborne, discrete airborne and discrete terrestrial laser scanning
773 data. *Forest Ecology and Management, 473*, 118268-118283

774 David, T.P., Herrick, J.E., & Abbott, L.B. (2010). A comparison of cover pole with
775 standard vegetation monitoring methods. *The Journal of Wildlife Management, 74*,
776 600-604

777 Davies, A.B., & Asner, G.P. (2014). Advances in animal ecology from 3D-LiDAR
778 ecosystem mapping. *Trends Ecol Evol, 29*, 681-691

779 Debus S. (2008) The effect of Noisy Miners on small bush birds: an unofficial cull
780 and its outcome. *Pacific Conservation Biology 14*, 185-190

781 Department of Environment, G.o.A. (2013). Vegetation Assessment Guide.

782 Dormann, C.F., Elith, J., Bacher, S., Buchmann, C., Carl, G., Carré, G., Marquéz,
783 J.R.G., Gruber, B., Lafourcade, B., Leitão, P.J., Münkemüller, T., McClean, C.,
784 Osborne, P.E., Reineking, B., Schröder, B., Skidmore, A.K., Zurell, D., &
785 Lautenbach, S. (2013). Collinearity: a review of methods to deal with it and a
786 simulation study evaluating their performance. *ECOGRAPHY, 36*, 27-46

787 Eldegard, K., Dirksen, J.W., Ørka, H.O., Halvorsen, R., Næsset, E., Gobakken, T., &
788 Ohlson, M. (2014). Modelling bird richness and bird species presence in a boreal
789 forest reserve using airborne laser-scanning and aerial images. *Bird Study, 61*, 204-
790 219

791 Fritz, A., Li, L., Storch, I. and Koch, B. (2018), UAV-derived habitat predictors
792 contribute strongly to understanding avian species–habitat relationships on the
793 Eastern Qinghai-Tibetan Plateau. *Remote Sensing of Ecology and Conservation,* 4,
794 53-65

795 Goetz, S., Steinberg, D., Dubayah, R., & Blair, B. (2007). Laser remote sensing of
796 canopy habitat heterogeneity as a predictor of bird species richness in an eastern
797 temperate forest, USA. *Remote Sensing of Environment, 108*, 254-263

798 Graf, R.F., Mathys, L., & Bollmann, K. (2009). Habitat assessment for forest dwelling
799 species using LiDAR remote sensing: Capercaillie in the Alps. *Forest Ecology and*
800 *Management, 257*, 160-167

801 Halstead, K.E., Alexander, J.D., Hadley, A.S., Stephens, J.L., Yang, Z., & Betts,
802 M.G. (2019). Using a species-centered approach to predict bird community
803 responses to habitat fragmentation. *Landscape Ecology, 34*, 1919-1935

804 Hartig, F. (2017). DHARMa: residual diagnostics for hierarchical (multi-level/mixed)
805 regression models. *R package version 0.1, 5*

Herrero-Huerta, M., Bucksch, A., Puttonen, E., & Rainey, K.M. (2020). Canopy Roughness: A New Phenotypic Trait to Estimate Aboveground Biomass from Unmanned Aerial System. *Plant Phenomics, 2020*, 6735967

Ikin, K., Knight, E., Lindenmayer, D. B., Fischer, J., Manning, A. D. (2012). Linking bird species traits to vegetation characteristics in a future urban development zone: implications for urban planning. *Urban Ecosystems,* 15**,** 961-977.

Isenburg, M. (2012). LAStools-efficient tools for LiDAR processing. *Available at: http: http://www.cs.unc.edu/~isenburg/lastools/*

James, F.C., & Shugart Jr, H.H. (1970). A quantitative method of habitat description. *Audubon Field Notes, 24*, 727-736

Jari Oksanen, F.G.B., Michael Friendly, Roeland Kindt, Pierre Legendre, Dan McGlinn, Peter R. Minchin, R. B. O'Hara, Gavin L. Simpson, Peter Solymos, M. Henry H. Stevens, Eduard Szoecs, Helene Wagner (2019). vegan: Community Ecology Package.

Karadimou, E.K., Kallimanis, A.S., Tsiripidis, I., & Dimopoulos, P. (2016). Functional diversity exhibits a diverse relationship with area, even a decreasing one. *Scientific Reports, 6*, 35420-35429

Kikkawa, J. (1982). Ecological association of birds and vegetation structure in wet tropical forests of Australia. *Australian Journal of Ecology, 7*, 325-345

Laliberté, E., & Legendre, P. (2010). A distance-based framework for measuring functional diversity from multiple traits. *Ecology, 91*, 299-305

LaRue, E.A., Wagner, F.W., Fei, S., Atkins, J.W., Fahey, R.T., Gough, C.M., & Hardiman, B.S. (2020). Compatibility of Aerial and Terrestrial LiDAR for Quantifying Forest Structural Diversity. *Remote Sensing, 12*, 1407-1421

Le Roux, D. S., Ikin, K., Lindenmayer, D. B., Manning, A. D., Gibbons, P. (2018). The value of scattered trees for wildlife: Contrasting effects of landscape context and tree size. 24**,** 69-81

Lee, P.S., Mackey, B.G., & Berry, S.L. (2017). Modelling vegetation structure-based bird habitat resources in Australian temperate woodlands, using multi-sensors. *European Journal of Remote Sensing, 46*, 641-674

Lefsky, M.A., Cohen, W.B., Parker, G.G., & Harding, D.J. (2002). Lidar Remote Sensing for Ecosystem Studies. *BioScience, 52*, 19-30

Lesak, A.A., Radeloff, V.C., Hawbaker, T.J., Pidgeon, A.M., Gobakken, T., & Contrucci, K. (2011). Modeling forest songbird species richness using LiDAR-derived measures of forest structure. *Remote Sensing of Environment, 115*, 2823-2835

Levick, S.R., Richards, A.E., Cook, G.D., Schatz, J., Guderle, M., Williams, R.J., Subedi, P., Trumbore, S.E., & Andersen, A.N. (2019). Rapid response of habitat structure and above-ground carbon storage to altered fire regimes in tropical savanna. *Biogeosciences, 16*, 1493-1503

Levick, S.R., Whiteside, T., Loewensteiner, D.A., Rudge, M., & Bartolo, R. (2021). Leveraging TLS as a Calibration and Validation Tool for MLS and ULS Mapping of Savanna Structure and Biomass at Landscape-Scales. *Remote Sensing, 13*

Liang, X., Kankare, V., Hyyppä, J., Wang, Y., Kukko, A., Haggrén, H., Yu, X., Kaartinen, H., Jaakkola, A., Guan, F., Holopainen, M., & Vastaranta, M. (2016).

Terrestrial laser scanning in forest inventories. *ISPRS Journal of Photogrammetry and Remote Sensing, 115*, 63-77

MacArthur, R., and J. MacArthur (1961). On bird species diversity. *Ecology, 42*, 594-598

Manning, A.D., Cunningham, R.B., & Lindenmayer, D.B. (2013). Bringing forward the benefits of coarse woody debris in ecosystem recovery under different levels of grazing and vegetation density. *Biological Conservation, 157*, 204-214

Manning, A.D., Lindenmayer, D.B., & Barry, S.C. (2004a). The conservation implications of bird reproduction in the agricultural "matrix": a case study of the vulnerable superb parrot of south-eastern Australia. *Biological Conservation, 120*, 363-374

Manning, A.D., Lindenmayer, D.B., & Nix, H.A. (2004b). Continua and Umwelt: novel perspectives on viewing landscapes. *OIKOS, 104*, 621-628

Manning, A.D., Wood, J.T., Gunningham, R.B., McIntyre, S., Shorthouse, D.J., Gordon, I.J., & Lindenmayer, D.B. (2011). Integrating research and restoration: the establishment of a long-term woodland experiment in south-eastern Australia. *Zoologist, 35*, 633-648

Mason, N.W.H., Mouillot, D., Lee, W.G., & Wilson, J.B. (2005). Functional richness, functional evenness and functional divergence: the primary components of functional diversity. *OIKOS, 111*, 112-118

McIntyre, S., Cunningham, R.B., Donnelly, C.F., & Manning, A.D. (2014). Restoration of eucalypt grassy woodland: effects of experimental interventions on ground-layer vegetation. *Australian Journal of Botany, 62*

McIntyre, S., Stol, J., Harvey, J., Nicholls, A.O., Campbell, A., Reid, A., Manning, A.D., Lindenmayer, D.B. (2010). Biomass and floristic patterns in the ground layer vegetation of box-gum grassy eucalypt woodland in Goorooyarroo and Mulligans Flat Nature Reserves, Australian Capital Territory. *Cunninghamia: a journal of plant ecology for eastern Australia, 11*, 319-357

Melin, M., Hinsley, S.A., Broughton, R.K., Bellamy, P., & Hill, R.A. (2018). Living on the edge: utilising lidar data to assess the importance of vegetation structure for avian diversity in fragmented woodlands and their edges. *Landscape Ecology, 33*, 895-910

Michel, P., Jenkins, J., Mason, N., Dickinson, K.J.M., & Jamieson, I.G. (2008). Assessing the ecological application of lasergrammetric techniques to measure fine-scale vegetation structure. *Ecological Informatics, 3*, 309-320

Montague-Drake, R.M., Lindenmayer, D.B., Cunningham, R.B., & Stein, J.A. (2011). A reverse keystone species affects the landscape distribution of woodland avifauna: a case study using the Noisy Miner (Manorina melanocephala) and other Australian birds. *Landscape Ecology, 26*, 1383-1394

Morris, E.K., Caruso, T., Buscot, F., Fischer, M., Hancock, C., Maier, T.S., Meiners, T., Müller, C., Obermaier, E., Prati, D., Socher, S.A., Sonnemann, I., Wäschke, N., Wubet, T., Wurst, S., & Rillig, M.C. (2014). Choosing and using diversity indices: insights for ecological applications from the German Biodiversity Exploratories. *Ecology and evolution, 4*, 3514-3524

Müller, J., Stadler, J., & Brandl, R. (2010). Composition versus physiognomy of vegetation as predictors of bird assemblages: The role of lidar. *Remote Sensing of Environment, 114*, 490-495

Nakagawa, S., Schielzeth, H., & O'Hara, R.B. (2013). A general and simple method for obtainingR2from generalized linear mixed-effects models. *Methods in Ecology and Evolution, 4*, 133-142

Nature Conservation Act 2014 (2021), Australian Capital Territory, https://www.legislation.act.gov.au/View/a/2014-59/current/html/2014-59.html

Olschofsky, K., Mues, V., & Köhl, M. (2016). Operational assessment of aboveground tree volume and biomass by terrestrial laser scanning. *Computers and Electronics in Agriculture, 127*, 699-707

Pretzsch, H. (2009). Description and Analysis of Stand Structures. In H. Pretzsch (Ed.), *Forest Dynamics, Growth and Yield: From Measurement to Model* (pp. 223-289). Berlin, Heidelberg: Springer Berlin Heidelberg

R Core Team (2020). R: A Language and Environment for Statistical Computing. . In. Vienna, Austria: R Foundation for Statistical Computing

Roussel, J. (2017). Auty, D. lidR: Airborne LiDAR Data Manipulation and Visualization for Forestry Applications. *R package version, 1*

Šašak, J., Gallay, M., Kaňuk, J., Hofierka, J., & Minár, J. (2019). Combined Use of Terrestrial Laser Scanning and UAV Photogrammetry in Mapping Alpine Terrain. *Remote Sensing, 11*, 2154

Sasaki, T., Imanishi, J., Fukui, W., & Morimoto, Y. (2016). Fine-scale characterization of bird habitat using airborne LiDAR in an urban park in Japan. *Urban Forestry & Urban Greening, 17*, 16-22

Seavy, N.E., Viers, J.H., & Wood, J.K. (2009). Riparian bird response to vegetation structure: a multiscale analysis using LiDAR measurements of canopy height. *Ecological Applications, 19*, 1848-1857

Sekercioglu, C.H. (2002). Effects of forestry practices on vegetation structure and bird community of Kibale National Park, Uganda. *Biological Conservation 107*, 229–240

Shokirov, S. (2021). Using multi-platform LiDAR to assess vegetation structure for woodland forest fauna In, *Research School of Biology* (p. 192). Australia: Australian National University

Shokirov, S., Levick, S.R., Jucker, T., Yeoh, P., & Youngentob, K. (2020). Comparison of TLS and ULS Data for Wildlife Habitat Assessments in Temperate Woodlands. In, *IGARSS 2020 - 2020 IEEE International Geoscience and Remote Sensing Symposium* (pp. 6097-6100)

Shorthouse, D.J., Iglesias, D., Jeffress, S., Lane, S., Mills, P., Woodbridge, G., McIntyre, S., & Manning, A.D. (2012). The 'making of' the Mulligans Flat - Goorooyarroo experimental restoration project. *Ecological Management & Restoration, 13*, 112-125

Soudarissanane, S., Lindenbergh, R., Menenti, M., & Teunissen, P. (2009). Incidence angle influence on the quality of terrestrial laser scanning points. In,

Proceedings ISPRS Workshop Laserscanning 2009, 1-2 Sept 2009, Paris, France: ISPRS

Stagoll, K., Manning, A.D., Knight, E., Fischer, J., & Lindenmayer, D.B. (2010). Using bird–habitat relationships to inform urban planning. *Landscape and Urban Planning, 98*, 13-25

Stanley, H.A., & Herman, H.S.J. (1974). Habitat Selection of Breeding Birds in an East Tennessee Deciduous Forest. *Ecology, 55*, 828-837

Sumnall, M.J., Hill, R.A., & Hinsley, S.A. (2016). Comparison of small-footprint discrete return and full waveform airborne lidar data for estimating multiple forest variables. *Remote Sensing of Environment, 173*, 214-223

SZ DJI TECHNOLOGY CO., L. (2018). DJI GS Pro User Manual. In

Val, J., Eldridge, D.J., Travers, S.K., Oliver, I., & Minderman, J. (2018). Livestock grazing reinforces the competitive exclusion of small-bodied birds by large aggressive birds. *Journal of Applied Ecology, 55*, 1919-1929

van Ewijk, K.Y., Treitz, P.M., & Scott, N.A. (2011). Characterizing Forest Succession in Central Ontario using Lidar-derived Indices. *Photogrammetric Engineering & Remote Sensing, 77*, 261-269

Venables, W.N., & Ripley, B.D. (2003). *Modern applied statistics with S*. New York: Springer Science & Business Media

Verschuyl, J.P., Hansen, A.J., McWethy, D.B., Sallabanks, R., & Hutto, R.L. (2008). Is the effect of forest structure on bird diversity modified by forest productivity? *Ecol Appl, 18*, 1155-1170

Vierling, K.T., Vierling, L.A., Gould, W.A., Martinuzzi, S., & Clawges, R.M. (2008). Lidar: shedding new light on habitat characterization and modeling. *Frontiers in Ecology and the Environment, 6*, 90-98

Weisberg, P.J., Dilts, T.E., Becker, M.E., Young, J.S., Wong-Kone, D.C., Newton, W.E., & Ammon, E.M. (2014). Guild-specific responses of avian species richness to LiDAR-derived habitat heterogeneity. *Acta Oecologica, 59*, 72-83

Wilkes, P., Lau, A., Disney, M., Calders, K., Burt, A., Gonzalez de Tanago, J., Bartholomeus, H., Brede, B., & Herold, M. (2017). Data acquisition considerations for Terrestrial Laser Scanning of forest plots. *Remote Sensing of Environment, 196*, 140-153

Yebra, M., Marselis, S., van Dijk, A., Cary, G., & Chen, Y. (2015). Using LiDAR for forest and fuel structure mapping: options, benefits, requirements and costs. In. Australia: Bushfire & Natural Hazards CRC

Zehm, A., Nobis, M., & Schwabe, A. (2003). Multiparameter analysis of vertical vegetation structure based on digital image processing. *Flora - Morphology, Distribution, Functional Ecology of Plants, 198*, 142-160

977

978

979

Appendix 1.

We conducted a pilot study in March 2018 to determine the best method to characterize the 96 X 1 ha (50 m X 200 m) experimental sites with TLS data to achieve the most complete coverage within a timeframe that would allow us to scan all of the sites within a month. We collected TLS data at 1.7m scanner height with 6 mm point spacing at 10 m distance from the scanner. Data were collected from 5, 6 and 7 scanning stations in a test site (Fig A1). These stations were established in a zigzag formation with approximately equal spacing between the stations to cover the 200 m x 50 m site. Data collection was performed with and without co-registering the scanning stations to determine whether co-registration during collection was more efficient than later co-registration during post-processing. Co-registration allows a surveyor to tie multiple scans in the same site together using targets directly in the field. However, this method requires more time to place and scan targets and could reduce the number of scan points within a site in a given timeframe (Liang et al., 2016b, Blakey et al., 2017). We found that data could be co-registered effectively during post-processing, and that allowed us to maximize the number of scans collected in the field.

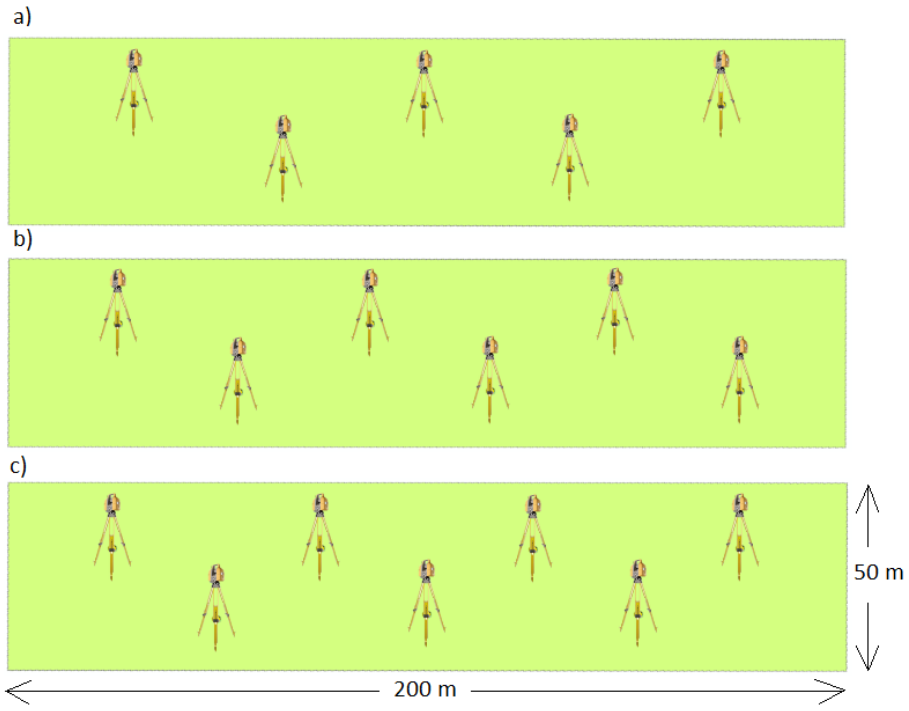

Figure A1. Test scan positions: a) 5 scans, b) 6 scans and c) 7 scans for 200 m by 50 m size sites.

Appendix 2. Contribution of TLS (left) and ULS (right) LiDAR variables for the first and the second PCA axis

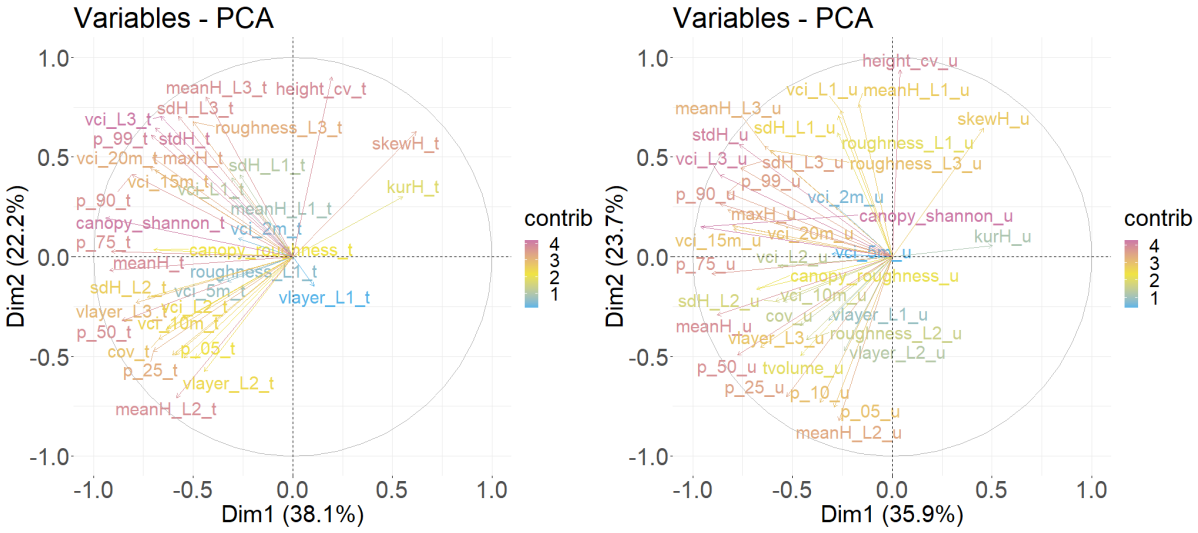

Appendix 3. Pearson correlation matrix of TLS variables

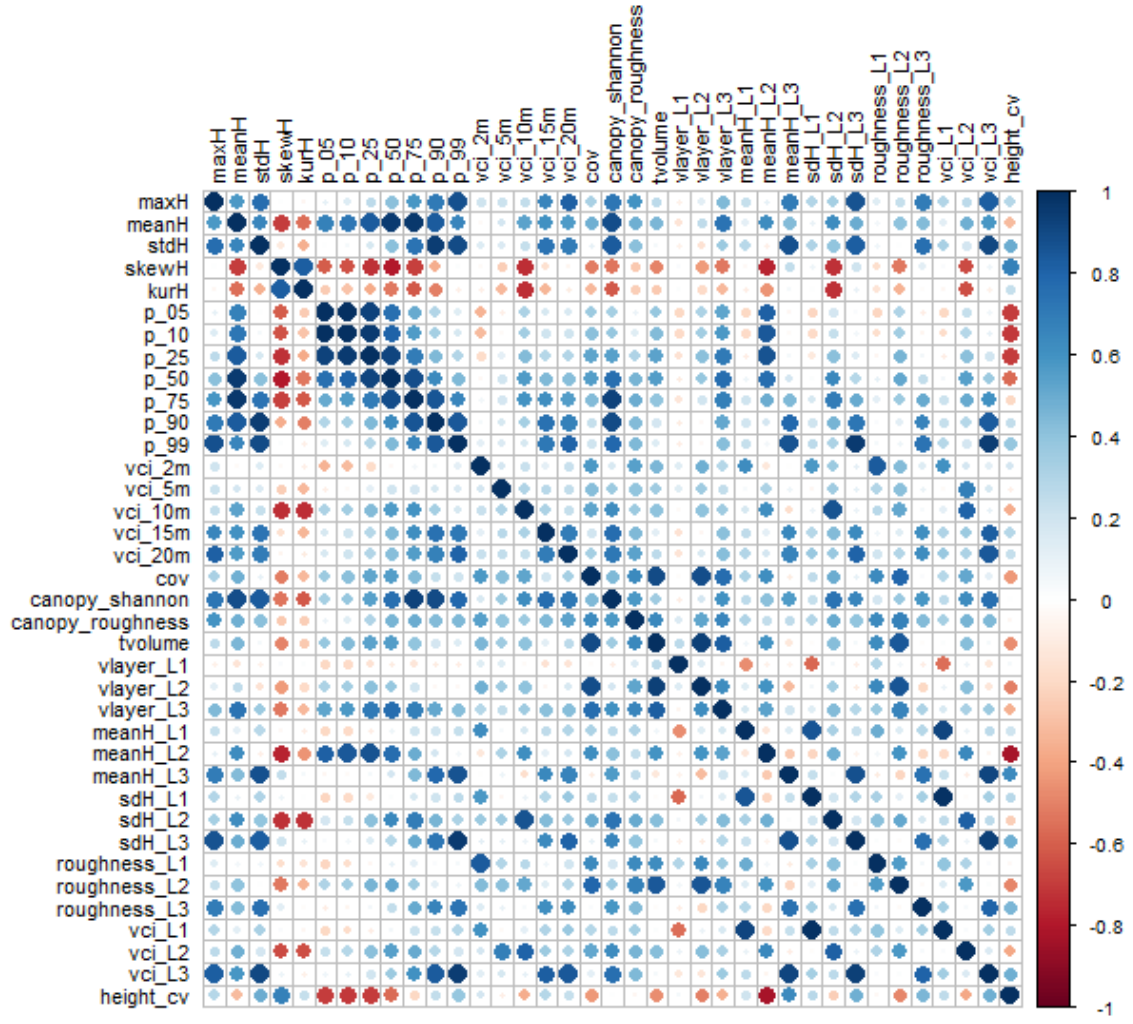

1005

1006 **Appendix 4. Pearson correlation matrix of ULS variables**

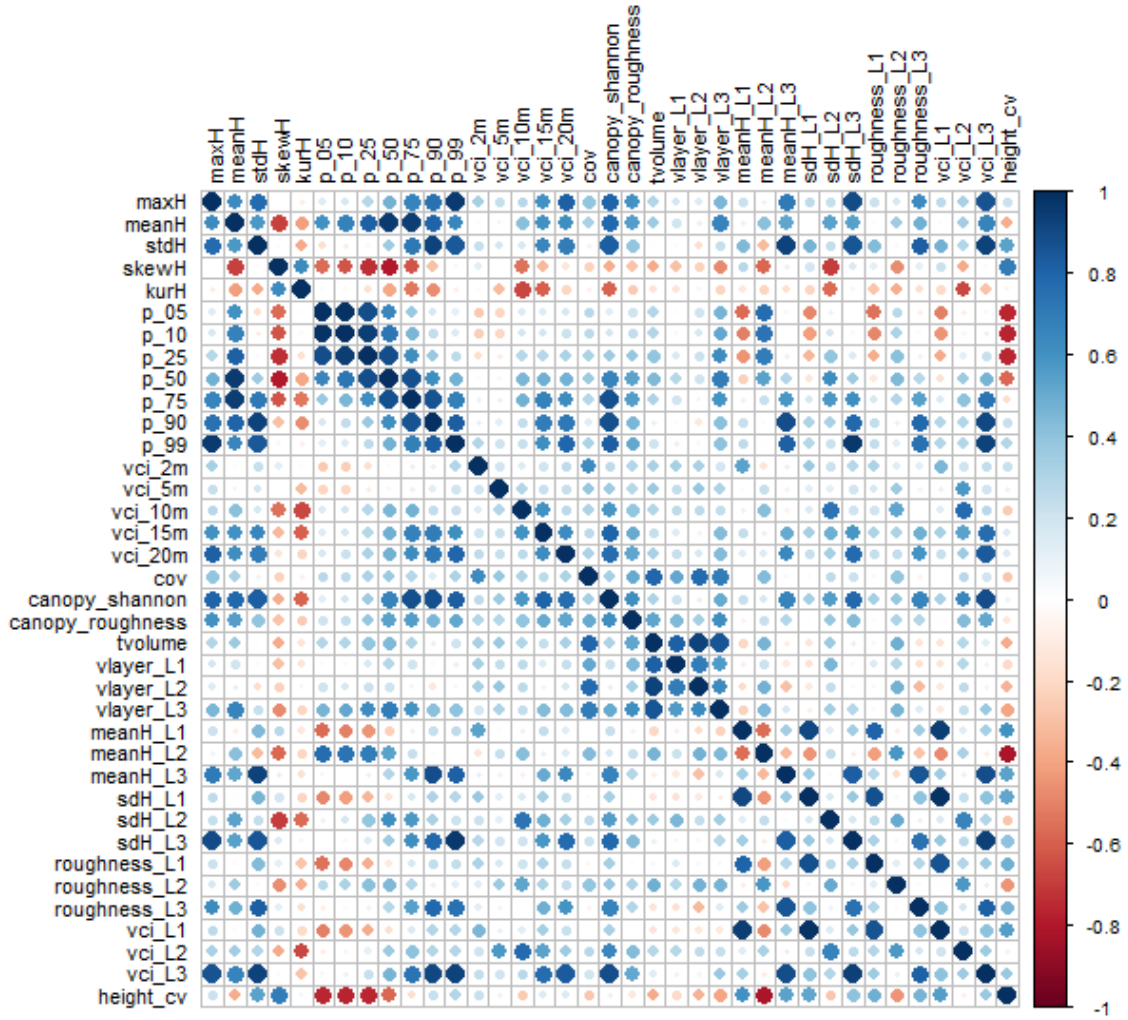

Appendix 5.

Table A5.1. Confusion matrix for vegetation classes predicted using terrestrial laser scanner (TLS) LiDAR variables. Vegetation classes are high tree high shrub (HTHS), high tree low shrub (HTLS), low tree high shrub (LTHS), and low tree low shrub (LTLS).

Vegetation classes were predicted from the first four PCA variables calculated from all TLS LiDAR variables					User's accuracy (%)	Vegetation classes were predicted from 12 selected TLS LiDAR variables				User's accuracy (%)
	HTHS	HTLS	LTHS	LTLS		HTHS	HTLS	LTHS	LTLS	
HTHS	21	5	6	4	58.3	26	5	6	3	65.0
HTLS	3	3	1	0	42.9	2	6	0	0	75.0
LTHS	6	5	9	0	45.0	1	3	9	3	56.3
LTLS	0	3	4	24	77.4	1	2	5	22	73.3
Producer's accuracy (%)	70.0	18.8	45.0	85.7		86.7	37.5	45.0	78.6	
Classification accuracy (%)	60.6					67.0				

Table A5.2. Confusion matrix of vegetation classes predicted using UAV laser scanner (ULS) LiDAR variables. Vegetation classes are high tree high shrub (HTHS), high tree low shrub (HTLS), low tree high shrub (LTHS), and low tree low shrub (LTLS).

Vegetation classes were predicted from the first four PCA variables calculated from ULS LiDAR variables					User's accuracy (%)	Vegetation classes were predicted from 12 selected ULS LiDAR variables				User's accuracy (%)
	HTHS	HTLS	LTHS	LTLS		HTHS	HTLS	LTHS	LTLS	
HTHS	24	4	13	3	54.5	25	3	4	1	75.8
HTLS	3	5	1	2	45.5	3	8	2	1	57.1
LTHS	3	3	1	0	14.3	1	4	11	3	57.9
LTLS	0	4	5	23	71.9	1	1	3	23	82.1
Producer's accuracy (%)	80.0	31.3	5.0	82.1		83.3	50.0	55.0	82.1	
Classification accuracy (%)	56.4					71.3				